

Oscillatory Josephson-Vortex Resistance in Stacks of $\text{Bi}_2\text{Sr}_2\text{CaCu}_2\text{O}_{8+x}$ Intrinsic Josephson Junctions

Jae-Hyun Choi^a, Myung-Ho Bae^a, Hu-Jong Lee^{*a} and Sang-Jae Kim^b

^aDepartment of Physics, Pohang University of Science and Technology, Pohang 790-784, Republic of Korea

^bDepartment of Mechatronics Engineering, Cheju National University, Jeju 690-756, Republic of Korea

Abstract

We report the oscillation of the Josephson vortex-flow resistance in the rectangular stacks of $\text{Bi}_2\text{Sr}_2\text{CaCu}_2\text{O}_{8+x}$ (Bi-2212) intrinsic Josephson junctions (IJJs). A piece of Bi-2212 single crystal containing a few tens of IJJs was sandwiched between two gold electrodes and fabricated into a rectangular shape with the typical lateral size of about $1.5 \times 10 \mu\text{m}^2$, using e-beam lithography and focused ion-beam etching techniques. In a tesla-range magnetic field applied in parallel with the junction planes, the oscillation of the Josephson vortex flow resistance was observed at temperatures near 60 K. The oscillation results from the interplay between the triangular Josephson vortex lattice and the potential barrier at the boundary of a single crystal. The oscillatory magnetoresistance for different bias currents, external magnetic fields, and the tilt-angles provides useful information on the dynamics of the coupled Josephson-vortex lattice system.

Keywords : Josephson vortex, Josephson vortex-flow resistance, oscillating tunneling magnetoresistance, boundary pinning potential

I. Introduction

In a high external magnetic field (H_{ext}) applied in parallel with the ab planes of layered superconductors such as $\text{Bi}_2\text{Sr}_2\text{CaCu}_2\text{O}_{8+x}$ (Bi-2212) single crystals, a triangular Josephson vortex lattice forms in insulating layers of intrinsic Josephson junctions (IJJs) stacked along the c axis. In a c -axis tunneling current bias, the Josephson vortex lattice is driven along the insulating layers [1]. The resulting Josephson vortex-flow resistance (JVFR) exhibits oscillations by the boundary potential effect at the stack edges [2]. Many studies on the oscillation of the JVFR have been made using the Josephson vortex lattice formed in the s-shaped geometry [3] as shown in Fig. 1(a).

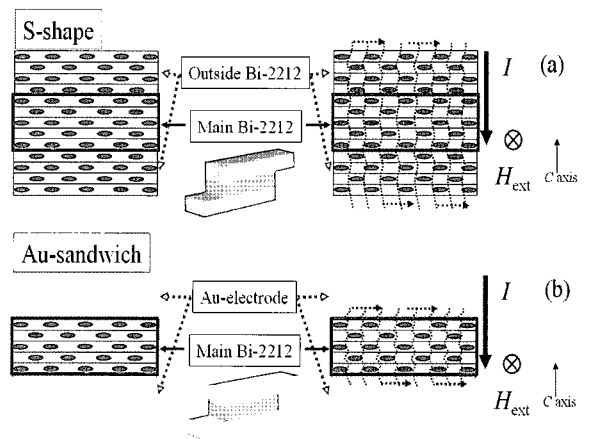


Fig. 1. Schematic geometry of the S-shaped and the Au-sandwiched Bi-2212 stack configurations. Fig. (a) depicts the coupling of Josephson vortices between the main sample stack and the outside basal stacks in the s-shaped geometry. Fig. (b) depicts the coupling of Josephson vortices only inside the sample stack of the Au-sandwiched geometry.

*Corresponding author. Fax : +82 54 279 5564
e-mail : hjlee@postech.ac.kr

In this s-shaped geometry, however, the strong Josephson vortex coupling is established between the main stack of IJJs under study and the stacks at the outside of it. The coupling of the Bi-2212 outside stacks may interfere with the pure boundary potential effect at the edges. Josephson vortex dynamics with the outside stacks eliminated have not been studied experimentally to date. In this study, using a stack without the outside stacks, we intended to observe the pure boundary potential effect at the edges. Our study using the ‘sandwich geometry’ sample, however, exhibits magnetoresistance characteristics, which are similar to the ones obtained using the s-shaped geometry samples. This implies that the boundary pinning interaction is much stronger than the interlayer coupling interaction, making the coupling between the main stack and the outside stacks not substantial.

II. Experiment

As-grown slightly underdoped Bi-2212 single crystals were prepared by the conventional solid-state-reaction method. A stack of IJJs was sandwiched between two Au-electrodes deposited on the top and the bottom of the stack using the double-side cleaving technique [4]. The sample was prepared by the e-beam lithography and the focused ion-beam (FIB) etching techniques. Details of the sample fabrication are described elsewhere [5]. Samples A and B are $10 \times 1.5 \times 0.02 \mu\text{m}^3$ and $14 \times 1.4 \times 0.05 \mu\text{m}^3$ in their length (l), width (w), and thickness (t), respectively.

The samples were cooled down to 60 K in a He⁴ cryostat with the sample mounting stage rotating with respect to the magnetic-field direction. We measured the c -axis JVFR by typical two-terminal DC measurements with room temperature low pass filters connected to the measurements leads. In-plane field alignment was done within the resolution of 0.01 degree, in a magnetic field of 3 T at 60 K [6].

In measurements, the oscillation of the JVFR was first confirmed by increasing the in-plane magnetic

field up to 3 T. The bias current dependence of the JVFR was then obtained by changing the c -axis bias current from 0.2 μA to 2.0 μA . The dependence of the JVFR on the magnetic field tilt-angle was also obtained for θ varying from 0.00° to 0.48° in a constant tunneling bias current of 1 μA .

III. Results and Discussion

The superconducting transition takes place at $T_c = 81$ K and 83 K for Samples A and B, respectively. The doping level δ of Bi-2212 crystal estimated using the relation with the tunneling resistance ratio ($r = R_c^{\text{max}}/R_c^{300\text{K}}$), $\delta = 0.174 + 0.321/(r + 1.932)$, with the room-temperature junction resistance $R_c^{300\text{K}} = 631 \Omega$ and the maximum resistance at T_c $R_c^{\text{max}} = 2215 \Omega$, was $\delta = 0.233$; slightly underdoped [7].

In the superconducting state a constant bias current along the c -axis drives Josephson vortices to the direction perpendicular to both the current and the external field when the field is applied in parallel with the ab -planes. The resulting motion of vortices causes the JVFR [1]. Fig. 2(a) shows the external field dependence of the JVFR of Sample A in various tunneling bias currents in the range of 0.2-2.0 μA .

The periodic oscillations were observed in all current biases. H_{start} (≈ 4.5 kOe) is the magnetic field value, where the JVFR becomes appreciable. H_{stop} (≈ 11.2 kOe), on the other hand, is the external magnetic field at which the oscillation amplitude of the JVFR vanishes. H_p (≈ 680 Oe) is the period of the oscillation of JVFR [see Fig. 2(b)]. As seen in Fig. 2(b), H_p is independent of current biases. Sample B shows similar JVFR as Sample A [the inset of Fig. 1(a)], but with the changed period of 510 Oe corresponding to the different width of 14 μm .

The magnetic field dependence of the JVFR for Sample A in Fig. 2(a) can be divided into three characteristic regions. Region I (0~2.3 kOe) corresponds to the Josephson vortex pinning state. The extent of this flat JVFR region is slightly sample-dependent and depends on the bias current density. The field-independence of the resistance is

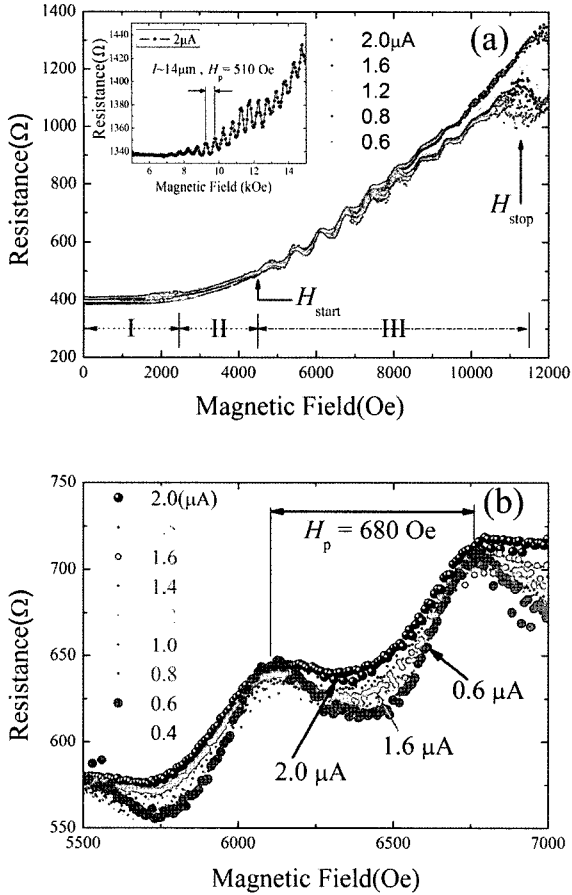


Fig. 2. Josephson vortex-flow resistance (JVFR) of Sample A versus magnetic fields in various bias currents in the range of 0.6–2.0 μA from bottom to top. (a) H_{start} and H_{stop} , defined in the text, are almost independent of the bias current. (b) Bias current dependencies of the amplitude of the resistance dips, which reflects the dynamic characteristics of Josephson vortices in a confined geometry. Inset of (a): the JVFR of Sample B in the bias of 2 μA .

most likely to be caused by pinning of Josephson vortices due to the boundary potential at the edge of each junction. The constant finite resistance in the region was from the lead and contact resistances in the two-probe measurement configuration. Region II (2.3–4.5 kOe) is believed to be the Josephson vortex liquid state, taking place by the random motion of the Josephson vortices as they are released from the boundary pinning potential. Region III (4.5–11.2 kOe) is the Josephson-vortex solid state. In this

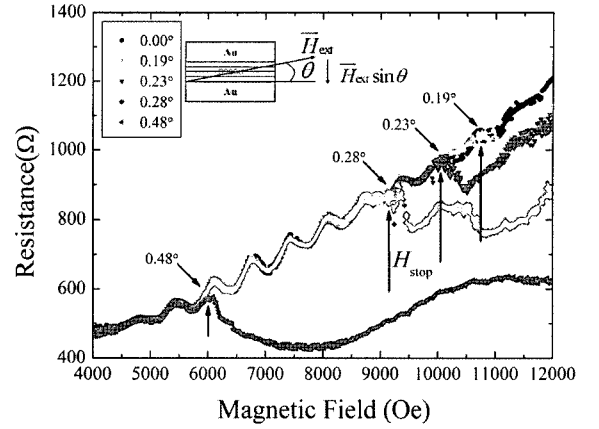


Fig. 3. The θ dependence of the vortex-flow resistance, where θ is the angle between the magnetic field and the ab planes of the sample (see the schematic configuration in the inset), which shows the θ dependence of H_{stop} .

region, Josephson vortices form a lattice structure, which is represented by the regular oscillation of the JVFR [2] as shown in Fig. 2(a). In higher magnetic fields above 11.2 kOe, their c -axis component due to a slight field misalignment along the ab plane may exceed the c -axis lower critical field H_{c1} for the entry of the Abrikosov pancake vortices. Josephson vortices are then pinned randomly by the pancake vortices at H_{stop} [2], with the vanishing oscillation but with a finite resistance. More discussion on H_{stop} is given below in relation with Fig. 3.

Fig. 2(b) shows oscillations with the period of $H_{p(\text{observed})}=680$ Oe, which is consistent with the predicted value, $H_p=\phi_0/2sl=690$ Oe, for the oscillatory JVFR of the triangular vortex lattice by the boundary potential. Here ϕ_0 ($=2.07 \times 10^{-7}$ G cm^2) is the flux quantum and s ($=1.5$ nm) is the thickness of an intrinsic Josephson junction in Bi-2212. The result shows that the period of the oscillation corresponds to the field needed to add “one” vortex quantum per “two” intrinsic Josephson junctions. Thus, Josephson vortices are supposed to form a triangular lattice in the ground state with the Josephson-vortex-flow resistance oscillation [2].

As shown in Fig. 2(b), the minimum of the current bias level depends on the bias current level. The phenomena can be explained by the dynamics of

Josephson vortices. The motion of Josephson vortices in a dip is limited by the pinning of the boundary potential. Then, the washboard-potential picture leads to higher depinning rate in higher bias current, leading to raising the dip resistance with increasing the bias current. In other words, the enhanced bias current increases the number of moving Josephson vortices freed from the boundary potential. On the other hand, at each maximum JVFR point Josephson vortex motion is in almost the vortex-flow state, where almost all the Josephson vortices are already in motion. The resulting voltage is linearly proportional to the bias current and the vortex number density. Thus, the JVFR, which is the vortex-flow voltage divided by the bias current, depends only on the vortex number density or on the external magnetic field as shown in Fig. 2(b).

Fig. 3 shows that the JVFR of Sample A depends on the tilt angle (θ), where θ is the angle between the magnetic field and the ab -plane as shown in the inset Fig. 3. We measured the JVFR as a function of θ , with θ varying from 0.00° to 0.48° (degree). The periodic oscillations were observed for θ up to $\pm 0.48^\circ$. Here, oscillation field H_p is insensitive to the tilt angle θ . As denoted by the vertical arrows, H_{stop} decreases with increasing θ . This is the general trend expected for the c -axis component of the magnetic field, because the c -axis component of H_{ext} causes

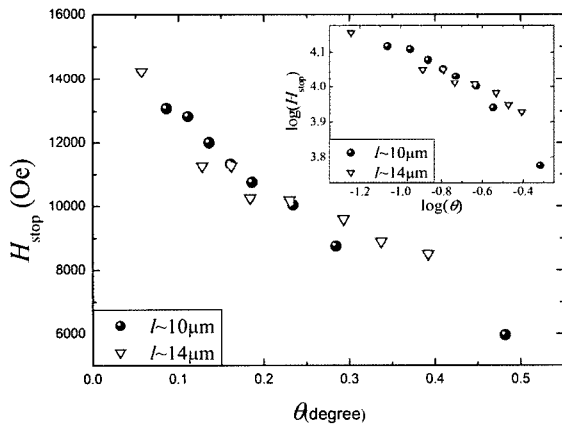


Fig. 4. The tilt-angle dependence of H_{stop} , which is slower than $1/\theta$ variation.

field-induced pancake vortices [8]. Therefore, we can express $H_{c1} \sim H_{\text{stop}} \cdot \sin\theta$ (H_{c1} is the critical field for the entry of the pancake vortices) [2]. When θ is very small ($\theta \ll 1$), the formula reads as $H_{c1} \sim H_{\text{stop}} \cdot \theta$ so that H_{stop} should be nearly proportional to $1/\theta$ with the coefficient of an order of H_{c1} . Fig. 4 shows the tilt-angle dependence of H_{stop} , which exhibits a power-law dependence on the tilt-angle θ . But, the θ dependence of H_{stop} is much slower than the simple-minded $1/\theta$ variation. This indicates that, in a higher tilt angle, the Josephson vortex lattice with a larger lattice constant for a smaller entry field of pancake vortices necessitates more pancake vortices for its lattice structure to be disturbed and thus, in turn, its oscillatory magnetoresistance behavior is diminished. The lower-density Josephson vortex lattice may have lower probability to be pinned down by the bias-generated planar pancake vortices.

Acknowledgments

This work was supported by the National Research Laboratory Program administered by Korea Science and Engineering Foundation.

References

- [1] M.-H. Bae and H.-J. Lee, "Dynamical transition of Josephson vortex lattice in serially stacked $\text{Bi}_2\text{Sr}_2\text{CaCu}_2\text{O}_{8+\delta}$ intrinsic Josephson junctions", *Progress in Superconductivity*, **6**, 52 (2004).
- [2] S. Ooi, T. Mochiku, and K. Hirata, "Periodic oscillations of Josephson-vortex flow resistance in $\text{Bi}_2\text{Sr}_2\text{CaCu}_2\text{O}_{8+\delta}$ ", *Phys. Rev. Lett.* **89**, 247002 (2002).
- [3] K. Hirata, S. Ooi, E. H. Sadki, and T. Mochiku, "Josephson vortex flow in $\text{Bi}_2\text{Sr}_2\text{CaCu}_2\text{O}_{8+\delta}$ ", *Physica B* **329-333**, 1332 (2003).
- [4] H. B. Wang, P. H. Wu and T. Yamashita, "Stacks of intrinsic Josephson junctions singled out from inside $\text{Bi}_2\text{Sr}_2\text{CaCu}_2\text{O}_{8+\delta}$ single crystals", *Appl. Phys. Lett.* **78**, 4010 (2001)
- [5] M.-H. Bae and H.-J. Lee, "Collective renounce modes

- of Josephson vortices in sandwiched stack of $\text{Bi}_2\text{Sr}_2\text{CaCu}_2\text{O}_{8+\delta}$ intrinsic Josephson junctions”, *Phys. Rev. B* **70**, 52506 (2004).
- [6] M.-H. Bae, H.-J. Lee, J. Kim, and K.-T. Kim, “Microwave distribution in stacked $\text{Bi}_2\text{Sr}_2\text{CaCu}_2\text{O}_{8+\delta}$ intrinsic Josephson junctions in a transmission-line geometry”, *Appl. Phys. Lett.* **83**, 2187 (2003).
- [7] M. Suzuki and T. Watanabe, “Discrimination of the superconducting gap from the pseudogap in $\text{Bi}_2\text{Sr}_2\text{CaCu}_2\text{O}_{8+\delta}$ by interlayer tunneling spectroscopy”, *Phys. Rev. Lett.* **85**, 4787 (2000).
- [8] A. E. Koshelev, “Josephson vortices and solitons inside pancake vortex lattice in layered superconductors”, *Phys. Rev. B* **68**, 094520 (2003).